Int. J. Solids Structures, 1965, Vol. 1, pp. 353 to 370. Pergamon Press Ltd. Printed in Great Britain

MOVING LOAD ON A FLEXIBLY SUPPORTED TIMOSHENKO BEAM

J. D. ACHENBACH and C. T. SUN

Northwestern University, Evanston, Illinois

Abstract—A uniform beam of infinite length is subjected to a force whose point of application moves with constant velocity over the beam. Solutions are obtained that are time invariant in a coordinate system moving with the load velocity. The supporting foundation includes damping effects. The influence of the damping coefficient and the load velocity on the beam response is studied. The limiting case of no damping is included and the various resonance effects are clarified.

NOTATION*

E	Young's modulus
I	moment of inertia of beam
ψ	rotation of cross-section
w	transverse displacement of beam (deflexion)
W	dimensionless transverse displacement of beam
x	distance along beam
v	velocity of the force
r	$= x - vt$
R	dimensionless r
A	cross-section of the beam
ρ	mass density of the beam
G	shear rigidity
$\varkappa'$	shear coefficient of a Timoshenko beam
q	foundation pressure/unit length
F_0	magnitude of the concentrated force
$\delta(\ )$	Dirac delta function
$H(\ )$	Heaviside unit function
η	coefficient of viscosity
k	spring constant
r_0	radius of gyration of the cross-section of the beam
ξ	damping ratio
a_1	thickness shear frequency ratio
a_2	extensional wave velocity ratio
θ	velocity parameter
β	$= \theta/a_1$
λ	$= a_2/a_1$
s	Fourier transform parameter
p	$= -is$
$\bar{\psi}, \bar{W}$	exponential Fourier transforms of ψ and W

* Additional symbols are defined as they occur in the text.

1. INTRODUCTION

IN SEVERAL FIELDS of engineering it has become of increasing interest to study the dynamics of beams supported by flexible foundations. An important class of problems in this area pertains to the response of a beam which is subjected to rapidly moving loads.

This paper is an investigation of the response of a Timoshenko beam to a force moving with constant velocity over the beam. The solutions are obtained under the assumption that the deformation is stationary relative to a coordinate system that moves with the load. Solutions of this type are sometimes referred to as 'steady-state' solutions. The beam is supported by a deformable foundation, but it is assumed that the foundation pressure at any point depends only on the deflexion and the transverse velocity at that point.

The 'steady-state' response of a Bernoulli–Euler beam on a purely elastic Winkler foundation has been studied by many authors. Solutions have been presented by Hovey [1] and later by Ludwig [2]. The problem was thoroughly reconsidered by Dörr [3], and again by Mathews [4]. The simplified beam and foundation models used in these papers limit their applicability. The Bernoulli–Euler beam cannot be applied at the increasing frequencies which result from higher load velocities. A significant improvement is obtained, however, by considering the Timoshenko beam, which takes into account the first mode of thickness-shear, and which is applicable at much higher frequencies. The 'steady-state' dynamic behavior of a Timoshenko beam on a purely elastic foundation has been studied by Crandall [5].

In the references [1–5] the Winkler assumption on the foundation was adopted. The Winkler assumption implies that the supporting continuum can be replaced by a set of parallel springs. This drastic simplification which includes neglecting the inertia of the foundation has been generally accepted. The Winkler foundation has also been used conjointly with a still more sophisticated beam theory (the exact theory) to study the propagation of wave trains [6].

For running load problems the elastic Winkler foundation gives rise to interesting resonance effects. For both the Bernoulli–Euler beam and the Timoshenko beam the amplitudes of the displacement, the rotation and the moment increase beyond bounds when the load velocity approaches a certain value, generally referred to as the critical velocity. For the case of the Timoshenko beam there are, moreover, two other load velocities for which a leading or a trailing resonance effect occurs. The latter resonance effects are fundamentally different from the first one in that not only the amplitudes of the displacement and the bending moment, but also the wave numbers of the rotation, the displacement and the bending moment increase beyond bounds. The terms leading and trailing resonance are used because the unlimited increases in amplitude and wave number take place either ahead of or behind the load. This particular character of the resonance at the second and the third critical speeds had not been recognized before. The second and the third critical velocities are respectively the propagation velocity of shear force disturbances $c_2 = (G\varkappa'/\rho)^{\frac{1}{2}}$ and the propagation velocity of moment disturbances $c_1 = (E/\rho)^{\frac{1}{2}}$. The first resonance effect, the one which occurs in the Bernoulli–Euler beam as well as in the Timoshenko beam, takes place at the minimum value of the phase velocity for free undeformed steady-state waves in the beam.

The present paper studies the influence of linear foundation damping on the 'steady-state' response of a Timoshenko beam. This problem is an extension of the work in [5] in that the springs of the elastic Winkler foundation have been replaced by viscoelastic Kelvin elements. The parameters in the present problem are the damping coefficient ξ and the load velocity parameter β. The different types of responses at various points in the ξ–β plane are studied and the results are presented in diagrams. Moreover, some additional information on the beam supported by the purely elastic foundation is obtained by considering it as a limit case $\xi \to 0$. The effect of linear damping was included for the Bernoulli–Euler beam by Kenney [7] and Mathews [8].

Analogous to the work reported in [1–8] are the investigations by several authors of the steady-state response of circular shells to ring loads. If axial displacements and longitudinal coupling are neglected thin shell theory yields a set of equations similar to the ones for the beam. In a recent paper [9] a simple shell bending theory with longitudinal coupling was utilized to study the steady-state response of a cylindrical shell to a moving ring load. The results of the present paper are pertinent to the same problem but in our paper rotatory inertia, transverse shear and damping are taken into account, while axial displacements and longitudinal coupling are neglected. Attention should also be drawn to work by Tang [10] who considered the response of a shell to a moving step load. He included rotatory inertia and transverse shear, but he did not include the effect of damping.

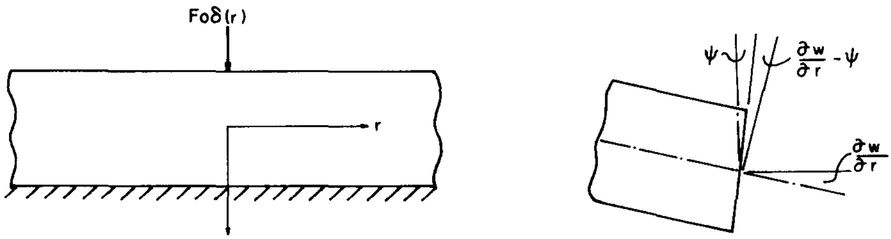

FIG. 1. Timoshenko beam on a flexible foundation.

2. FORMULATION OF THE PROBLEM

Timoshenko's equations for the displacement w and the rotation ψ of a freely vibrating beam with constant cross-sectional area A, moment of inertia I, mass density ρ, Young's modulus E, shear modulus G and shear coefficient $\varkappa'$ are (Fig. 1):

$$EI\frac{\partial^2\psi}{\partial x^2}+\varkappa' AG\left(\frac{\partial w}{\partial x}-\psi\right) = \rho I\frac{\partial^2\psi}{\partial t^2} \tag{1}$$

$$\varkappa' AG\left(\frac{\partial^2 w}{\partial x^2}-\frac{\partial\psi}{\partial x}\right) = \rho A\frac{\partial^2 w}{\partial t^2}. \tag{2}$$

If the beam is supported by a Winkler-type foundation and under the action of a force distribution $F(x, t)$, equation (2) becomes

$$\varkappa' AG\left(\frac{\partial^2 w}{\partial x^2}-\frac{\partial\psi}{\partial x}\right)+F(x, t)-q(x, t) = \rho A\frac{\partial^2 w}{\partial t^2} \tag{3}$$

where $q(x, t)$ is the restoring force from the foundation. In the present paper we consider a Winkler foundation with simple damping. The damping in the foundation is introduced by replacing the springs of the elastic Winkler foundation by viscoelastic Kelvin models, which consist of a spring placed parallel to a dashpot. For such a foundation the restoring force $q(x, t)$ can be expressed as

$$q = kw+\eta\frac{\partial w}{\partial t}. \tag{4}$$

The present case also applies if the foundation is elastic, but the damping is provided by other external mechanisms. The constant k is the foundation modulus and η is the damping coefficient.

The equations (1), (3) and (4) govern the displacements of the elastic beam on the damped (viscoelastic) foundation. If the applied load $F(x, t)$ is a constant force of magnitude F_0, which moves with constant velocity v over the beam it can be expressed as

$$F(x, t) = F_0\delta(x-vt) \tag{5}$$

where $\delta(\ )$ is the Dirac-delta function.

To facilitate the solution of equations (1), (3) and (4) we employ a transformation of variables which is suggested by physical considerations. Let us consider the displacement of the beam at a point which is at a specified distance r from the point of application of the force and whose position is therefore advancing in the positive x-direction with velocity v. We now assume that transient effects have died out and that a steady state has been reached. As a consequence of these assumptions the displacement only depends on r. The following transformation of coordinates is thus introduced

$$r = x-vt. \tag{6}$$

Considering the dependent variables to be functions of r only, we obtain from equations (1), (3), (4) and (5):

$$EI\frac{d^2\psi}{dr^2}+\varkappa' AG\left(\frac{dw}{dr}-\psi\right) = \rho I v^2\frac{d^2\psi}{dr^2} \tag{7}$$

$$\varkappa' AG\left(\frac{d^2w}{dr^2}-\frac{d\psi}{dr}\right)-q-\rho A v^2\frac{d^2w}{dr^2} = -F_0\delta(r) \tag{8}$$

$$q = kw-\eta v\frac{dw}{dr}. \tag{9}$$

The equations can be made dimensionless by measuring lengths in terms of the radius of gyration of the cross section and measuring time in terms of the period of vibration of the undeformed beam bouncing on the elastic foundation. We introduce

$$\begin{aligned} &r_0 = \sqrt{(I/A)} && \omega_0 = \sqrt{(k/\rho A)} && v_0 = r_0\omega_0 \\ &\xi = \eta/2\sqrt{(k\rho A)} && W = w/r_0 && R = r/r_0 \\ &\theta = v/v_0 && a_1 = \sqrt{(\varkappa' G/\rho)}/v_0 && a_2 = \sqrt{(E/\rho)}/v_0. \end{aligned} \tag{10}$$

Substitution of (10) into equations (7), (8) and (9) gives the dimensionless equations of motion

$$(a_2^2-\theta^2)\frac{d^2\psi}{dR^2}-a_1^2\psi+a_1^2\frac{dW}{dR} = 0 \tag{11}$$

$$(a_1^2-\theta^2)\frac{d^2W}{dR^2}+2\theta\xi\frac{dW}{dR}-W-a_1^2\frac{d\psi}{dR} = -F^*\delta(R) \tag{12}$$

where

$$F^* = F_0/r_0^2k.$$

3. APPLICATION OF THE COMPLEX FOURIER TRANSFORM

Solutions for the displacement W and the rotation ψ may be obtained with the Fourier transform technique. In the present paper the following pair of transforms has been used

$$\overline{f(s)} = \int_{-\infty}^{\infty} f(R)e^{-isR}\,dR \tag{13}$$

and

$$f(R) = \frac{1}{2\pi}\int_{-\infty}^{\infty} \overline{f(s)}e^{isR}\,ds. \tag{14}$$

Operating on (11) and (12) with the exponential Fourier transform we obtain

$$[-(a_2^2-\theta^2)s^2-a_1^2]\bar{\psi}+a_1^2is\overline{W} = 0 \tag{15}$$

$$[-(a_1^2-\theta^2)s^2+2\theta\xi is-1]\overline{W}-a_1^2is\bar{\psi} = -F^*. \tag{16}$$

The transformed displacement $\overline{W}$ and the transformed rotation $\bar{\psi}$ can now be solved from (15) and (16). The results are

$$\frac{\bar{\psi}}{F^*} = \frac{is}{a_1^2(1-\beta^2)(\lambda^2-\beta^2)s^4-2a_1\beta\xi(\lambda^2-\beta^2)is^3+(\lambda^2-\beta^2-a_1^2\beta^2)s^2-2a_1\xi\beta is+1} \tag{17}$$

$$\frac{\overline{W}}{F^*} = \frac{(\lambda^2-\beta^2)s^2+1}{a_1^2(1-\beta^2)(\lambda^2-\beta^2)s^4-2a_1\beta\xi(\lambda^2-\beta^2)is^3+(\lambda^2-\beta^2-a_1^2\beta^2)s^2-2a_1\xi\beta is+1}. \tag{18}$$

In (17) and (18) the following substitutions have been used

$$\theta = \beta a_1 \qquad a_2 = \lambda a_1. \tag{19}$$

It is noticed that the denominators of equation (17) and (18) are fourth order polynomials in s with real and imaginary coefficients. The biquadratic equation which results from equating this denominator to zero will henceforth be called the characteristic equation. The process of determining the inverse transform of $\bar{\psi}(s)$ and $\overline{W}(s)$ can be accomplished by elementary means, i.e., with a table of complex Fourier transforms, if we know the roots of the characteristic equation. The next section is devoted to a thorough investigation of the type of roots that occur for various combinations of the load velocity and damping parameters. Once the roots have been determined the functions $\bar{\psi}(s)$ and $\overline{W}(s)$ can be expanded into partial fractions. This process is straightforward and results in both cases in a sum of four terms, each of them of the general form $C/(s+b+ic)$, where C, b and c have constant or sometimes zero values. The inverse transforms of $\bar{\psi}(s)$ and $\overline{W}(s)$ can now be determined by noting that the inverse of

$$\frac{1}{s+b+ic} \text{ is } -\text{sgn}(c)ie^{cR}e^{-ibR}H[-R\,\text{sgn}(c)]. \tag{20}$$

In equation (20), sgn (c) and $H(R)$ are generalized functions defined by

$$\operatorname{sgn}(c) = \begin{cases} 1 & \text{for } c > 0 \\ -1 & \text{for } c < 0 \end{cases} \tag{21}$$

and

$$H(R) = \begin{cases} 1 & \text{for } R > 0 \\ 0 & \text{for } R < 0. \end{cases} \tag{22}$$

4. THE ROOTS OF THE CHARACTERISTIC EQUATION

The characteristic equation is a fourth order equation in s with real and imaginary coefficients. It is however easier to consider an equation with real coefficients and for that reason the substitution $s = ip$ is introduced; the result is

$$a_1^2(1-\beta^2)(\lambda^2-\beta^2)p^4 - 2a_1\beta\xi(\lambda^2-\beta^2)p^3 - (\lambda^2-\beta^2-a_1^2\beta^2)p^2 + 2a_1\xi\beta p + 1 = 0. \tag{23}$$

Inspection of equation (23) shows that for $\xi > 0$ the roots cannot be purely imaginary, and hence $\bar{\psi}(s)$ and $\bar{w}(s)$ cannot have poles on the real axis. To investigate the type of roots, i.e. real or complex, of equation (23) we have to consider the general discriminant of the equation. It is shown in, for example, [11] that the signs of the discriminant Δ determine the type of roots of the biquadratic equation. According to [11] the equation possesses two real and two imaginary roots if $\Delta < 0$. If on the other hand $\Delta > 0$ the roots are either all real or all complex. The roots are all real if two subdiscriminants P and Q are both negative.

After substitution of numerical values for a_1^2 and λ, the discriminant Δ is a function of the velocity parameter β and the damping parameter ξ. A careful investigation of the equation $\Delta = 0$ reveals that the equation is satisfied along certain curves in the first quadrant of the $\xi-\beta$ plane. It can be shown that $\Delta = 0$ along the line $\beta = \lambda$ and at the point $\xi = 0$, $\beta = a_0/a_1$. The discriminant is moreover equal to zero along two curves

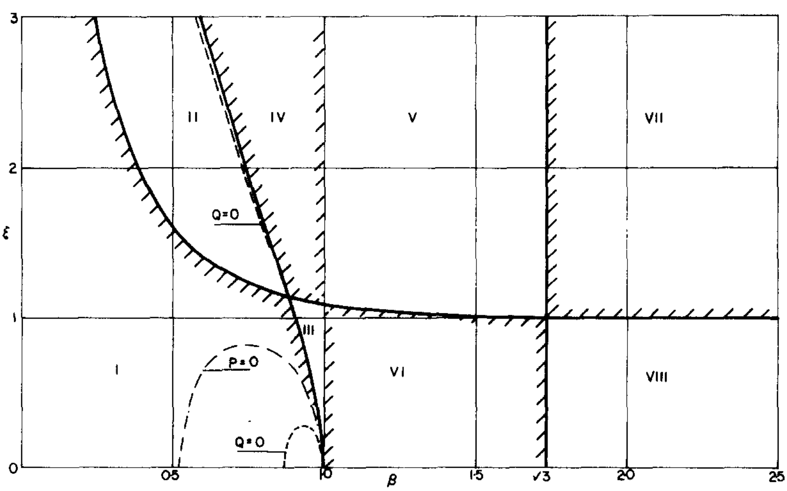

FIG. 2. Regions for roots of the characteristic equation, $a_1^2 = 10$, $\lambda^2 = 3$.

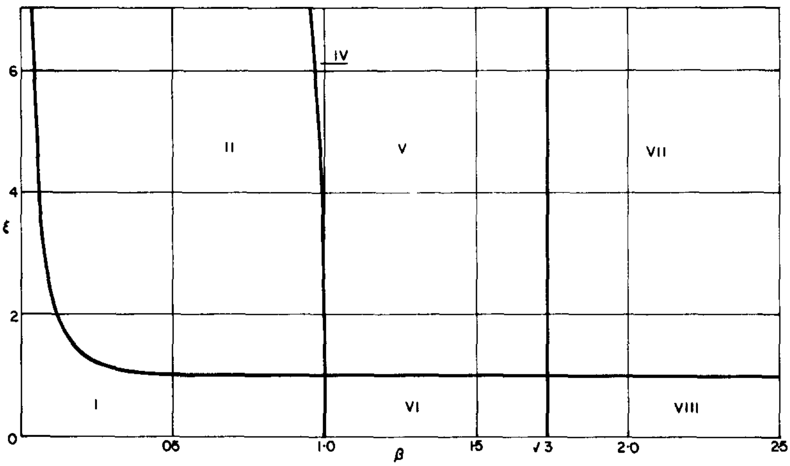

FIG. 3. Regions for roots of the characteristic equation, $a_1^2 = 1000$, $\lambda^2 = 3$.

which are shown for different values of a_1^2 in Fig. 2 and Fig. 3. The curves for which $\Delta = 0$ bound regions where Δ is positive or negative. In the regions of positive Δ the signs of P and Q determine whether the roots are all real or all complex. The curves $P = 0$ and $Q = 0$ have also been plotted in Fig. 2. The signs of P and Q can only change across the curves $P = 0$ and $Q = 0$, and these curves therefore bound regions of positive and negative P and Q. By testing it was determined that the regions of positive Δ are I, IV, V and VIII, Fig. 2. A check disclosed that only in the regions IV and V the conditions $P < 0$ and $Q < 0$ were met, and as a consequence we have four real roots in regions IV and V. The roots in the regions I and VIII are thus all complex.

From equation (20) it is seen that a root for s only contributes to the solution ahead of the load (head wave) if the imaginary part of the root is positive. As $s = ip$, a root of equation (23) only contributes to the head wave if the real part is positive. Similarly a root of equation (23) only contributes to the solution behind the load (tail wave) if the real part is negative. The signs of the real parts of the complex roots or the signs of the real roots can be determined with a technique which was developed by Routh [12]. Following Routh's method the number of positive real parts is equal to the number of sign changes of a sequence of test functions.

The results of the foregoing discussion are tabulated in Table 1. For every region of the first quadrant of the β–ξ plane, Fig. 2 and Fig. 3, the type of root of equation (23)

TABLE 1. TYPE OF ROOTS OF THE CHARACTERISTIC EQUATION

Region	Type of roots (p)	Type of roots (s)
I	$m_1 \pm in_1,\ -m_2 \pm in_2$	$\pm n_1 + im_1,\ \pm n_2 - im_2$
II	$m_1 \pm in_1,\ -m_2,\ -m_3$	$\pm n_1 + im_1,\ -im_2,\ -im_3$
III	$-m_1 \pm in_1,\ m_2,\ m_3$	$\pm n_1 - im_1,\ im_2,\ im_3$
IV	$-m_1,\ -m_2,\ m_3,\ m_4$	$-im_1,\ -im_2,\ im_3,\ im_4$
V	$-m_1,\ -m_2,\ -m_3,\ m_4$	$-im_1,\ -im_2,\ -im_3,\ im_4$
VI	$-m_1 \pm in_1,\ -m_2,\ m_3$	$\pm n_1 - im_1,\ -im_2,\ im_3$
VII	$-m_1 \pm in_1,\ -m_2,\ -m_3$	$\pm n_1 - im_1,\ -im_2,\ -im_3$
VIII	$-m_1 \pm in_1,\ -m_2 \pm in_2$	$\pm n_1 - im_1,\ \pm n_2 - im_2$

is shown as well as the sign of the real parts. The corresponding roots for s are listed in the last column.

In both Fig. 2 and Fig. 3 we used $\lambda = \sqrt{3}$. The values for a_1^2 were 10 and 1000 for Fig. 2 and Fig. 3 respectively. From the expressions given by (10) we can deduce the following form for a_2

$$a_2 = \tfrac{1}{2}\sqrt{(4EI/k)/r_0^2}. \tag{24}$$

From equation (24) it follows that a high value of a_2 corresponds to a stiff beam or a soft foundation.

5. SOLUTIONS FOR THE DISPLACEMENT $W(R)$ AND THE ROTATION $\psi(R)$

It is observed from Table 1 that the four roots of the characteristic equation can be four complex, two complex and two imaginary and four imaginary. In this section $\psi(R)$ and $W(R)$ are given for these three cases. The inverse transforms were obtained by expanding $\bar{\psi}(s)$ and $\bar{W}(s)$ into partial fractions and inverting the individual terms with equation (20).

Case 1. In the regions I and VIII roots of the general type: $s = \pm n_1 + im_1, \pm n_2 + im_2$. The following functions are defined

$$K(u, v) = \operatorname{sgn}(u)e^{-uR}\sin(vR)H[\operatorname{sgn}(u)R] \tag{25}$$

$$M(u, v) = \operatorname{sgn}(u)e^{-uR}\cos(vR)H[\operatorname{sgn}(u)R] \tag{26}$$

where sgn(u) and $H[\;]$ are defined by equations (21) and (22). Inverting (17) results in

$$\frac{a_1^2}{F^*}\psi = -\frac{2E_3}{E_1}K(m_1, n_1) - \frac{2E_2}{E_1}M(m_1, n_1) - \frac{2F_3}{F_1}K(m_2, n_2) - \frac{2F_2}{F_1}M(m_2, n_2). \tag{27}$$

The inverse transform of (18) is

$$\frac{a_1^2}{F^*}W = -\frac{2G_3}{G_1}K(m_1, n_1) - \frac{2G_2}{G_1}M(m_1, n_1) - \frac{2H_3}{H_1}K(m_2, n_2) - \frac{2H_2}{H_1}M(m_2, n_2). \tag{28}$$

The constants E, F, G and H are

$$E_1 = 2n_1\{[(m_1-m_2)^2-(n_1^2-n_2^2)]^2+4n_1^2(m_1-m_2)^2\}(1-\beta^2)(\lambda^2-\beta^2) \tag{29}$$

$$E_2 = 2m_1n_1(m_1-m_2)-n_1[(m_1-m_2)^2-(n_1^2-n_2^2)] \tag{30}$$

$$E_3 = m_1[(m_1-m_2)^2-(n_1^2-n_2^2)]+2n_1^2(m_1-m_2) \tag{31}$$

$$F_1 = 2n_2\{[(m_1-m_2)^2+(n_1^2-n_2^2)]^2+4n_2^2(m_1-m_2)^2\}(1-\beta^2)(\lambda^2-\beta^2) \tag{32}$$

$$F_2 = 2m_2n_2(m_2-m_1)-n_2[(m_1-m_2)^2+(n_1^2-n_2^2)] \tag{33}$$

$$F_3 = m_2[(m_1-m_2)^2+(n_1^2-n_2^2)]+2n_2^2(m_2-m_1) \tag{34}$$

$$G_1 = E_1 \tag{35}$$

$$G_2 = -2n_1(m_1-m_2)[1-(\lambda^2-\beta^2)(m_1^2-n_1^2)]-2m_1n_1(\lambda^2-\beta^2)[(m_1-m_2)^2-(n_1^2-n_2^2)] \tag{36}$$

$$G_3 = -[1-(\lambda^2-\beta^2)(m_1^2-n_1^2)][(m_1-m_2)^2-(n_1^2-n_2^2)]+4m_1n_1^2(\lambda^2-\beta^2)(m_1-m_2) \tag{37}$$

$$H_1 = F_1 \tag{38}$$

$$H_2 = 2n_2(m_1-m_2)[1-(\lambda^2-\beta^2)(m_2^2-n_2^2)]-2m_2n_2(\lambda^2-\beta^2)[(m_1-m_2)^2+(n_1^2-n_2^2)] \tag{39}$$

$$H_3 = -[1-(\lambda^2-\beta^2)(m_2^2-n_2^2)][(m_1-m_2)^2+(n_1^2-n_2^2)]-4m_2n_1^2(\lambda^2-\beta^2)(m_1-m_2). \tag{40}$$

Case 2. In the regions II, III, VI and VII, roots of the general type: $s = \pm n_1+im_1$, im_2, im_3. We define the function $N(u)$ as

$$N(u) = \operatorname{sgn}(u)e^{-uR}H[\operatorname{sgn}(u)R]. \tag{41}$$

The solution for the rotation is

$$\frac{a_1^2}{F^*}\psi = -\frac{2E_3'}{E_1'}K(m_1,n_1)-\frac{2E_2'}{E_1'}M(m_1,n_1)-F_1'N(m_2)-F_2'N(m_3). \tag{42}$$

The deflexion is given as

$$\frac{a_1^2}{F^*}W = -\frac{2G_3'}{G_1'}K(m_1,n_1)-\frac{2G_2'}{G_1'}M(m_1,n_1)-H_1'N(m_2)-H_2'N(m_3) \tag{43}$$

where the constants E', F', G' and H' are defined as

$$E_1' = 2n_1\{[(m_1-m_2)(m_1-m_3)-n_1^2]^2+n_1^2(2m_1-m_2-m_3)^2\}(1-\beta^2)(\lambda^2-\beta^2) \tag{44}$$

$$E_2' = m_1n_1(2m_1-m_2-m_3)-n_1[(m_1-m_2)(m_1-m_3)-n_1^2] \tag{45}$$

$$E_3' = m_1[(m_1-m_2)(m_1-m_3)-n_1^2]+n_1^2(2m_1-m_2-m_3) \tag{46}$$

$$F_1' = \frac{-m_2}{(m_2-m_3)[(m_1-m_2)^2+n_1^2](1-\beta^2)(\lambda^2-\beta^2)} \tag{47}$$

$$F_2' = \frac{-m_3}{(m_3-m_2)[(m_1-m_3)^2+n_1^2](1-\beta^2)(\lambda^2-\beta^2)} \tag{48}$$

$$G_1' = E_1' \tag{49}$$

$$G_2' = -2m_1n_1(\lambda^2-\beta^2)[(m_1-m_2)(m_1-m_3)-n_1^2]-n_1(2m_1-m_2-m_3)[1-(\lambda^2-\beta^2)(m_1^2-n_1^2)] \tag{50}$$

$$G_3' = 2m_1n_1^2(\lambda^2-\beta^2)(2m_1-m_2-m_3)-[1-(\lambda^2-\beta^2)(m_1^2-n_1^2)][(m_1-m_2)(m_1-m_3)-n_1^2] \tag{51}$$

$$H_1' = \frac{F_1'}{m_2}[(\lambda^2-\beta^2)m_2^2-1] \tag{52}$$

$$H_2' = \frac{F_2'}{m_3}[(\lambda^2-\beta^2)m_3^2-1]. \tag{53}$$

Case 3. In the regions, IV and V, roots of the general type: $s = im_1$, im_2, im_3, im_4. The inverse transform of the rotation is

$$\frac{a_1^2}{F^*}\psi = -E_1''N(m_1)-E_2''N(m_2)-E_3''N(m_3)-E_4''N(m_4). \tag{54}$$

The solution for the deflexion is

$$\frac{a_1^2}{F^*}W = -G_1''N(m_1)-G_2''N(m_2)-G_3''N(m_3)-G_4''N(m_4). \tag{55}$$

The constants E'' and G'' are

$$E_1'' = \frac{-m_1}{(m_1-m_2)(m_1-m_3)(m_1-m_4)(1-\beta^2)(\lambda^2-\beta^2)} \tag{56}$$

$$E_2'' = \frac{-m_2}{(m_2-m_1)(m_2-m_3)(m_2-m_4)(1-\beta^2)(\lambda^2-\beta^2)} \tag{57}$$

$$E_3'' = \frac{-m_3}{(m_3-m_1)(m_3-m_2)(m_3-m_4)(1-\beta^2)(\lambda^2-\beta^2)} \tag{58}$$

$$E_4'' = \frac{-m_4}{(m_4-m_1)(m_4-m_2)(m_4-m_3)(1-\beta^2)(\lambda^2-\beta^2)} \tag{59}$$

$$G_1'' = \frac{E_1''}{m_1}[(\lambda^2-\beta^2)m_1^2-1] \tag{60}$$

$$G_2'' = \frac{E_2''}{m_2}[(\lambda^2-\beta^2)m_2^2-1] \tag{61}$$

$$G_3'' = \frac{E_3''}{m_3}[(\lambda^2-\beta^2)m_3^2-1] \tag{62}$$

$$G_4'' = \frac{E_4''}{m_4}[(\lambda^2-\beta^2)m_4^2-1]. \tag{63}$$

6. THE DAMPING COEFFICIENT APPROACHING ZERO IN THE LIMIT

The special case of zero damping coefficient, that is when the beam is supported by an elastic Winkler foundation, is a limiting case of the formulation that was presented in the previous sections. The solutions for the elastically supported beam can be derived from equations (27), (28), (42) and (43), if appropriate care is exercised.

For $\xi = 0$ the biquadratic equation in s simplifies to

$$a_1^2(1-\beta^2)(\lambda^2-\beta^2)s^4+(\lambda^2-\beta^2-a_1^2\beta^2)s^2+1 = 0. \tag{64}$$

The solutions of equation (64) are

$$s = \pm\{[(a_1^2\beta^2-\lambda^2+\beta^2)\pm J^{\frac{1}{2}}]/2a_1^2(1-\beta^2)(\lambda^2-\beta^2)\}^{\frac{1}{2}} \tag{65}$$

where

$$J = (\lambda^2-\beta^2-a_1^2\beta^2)^2-4a_1^2(1-\beta^2)(\lambda^2-\beta^2). \tag{66}$$

Let a_0/a_1 be the positive real root of the equation $J = 0$. It is then easily shown that $J < 0$ and $J > 0$ for respectively $\beta < a_0/a_1$ and $\beta > a_0/a_1$. For values of a_1 of physical significance we find $a_0 < a_1$ and $\lambda > 1$, hence $a_0/a_1 < 1 < \lambda$. It can then be deduced from equation (65) that the roots of equation (64) are of the form:

$$0 < \beta < a_0/a_1 \qquad s = \pm n+im, \quad \pm n-im \tag{67a}$$

$$\beta = a_0/a_1 \qquad \text{double roots } s = \pm n, \quad \pm n \tag{67b}$$

$$a_0/a_1 < \beta < 1 \qquad s = \pm n_1, \quad \pm n_2 \tag{67c}$$

$$1 < \beta < \lambda \qquad s = \pm im, \quad \pm n \tag{67d}$$

$$\lambda < \beta \qquad s = \pm n_1, \quad \pm n_2. \tag{67e}$$

The deflexions and the rotations in the various β-regions can be obtained in the following manner

(1) $0 < \beta < a_0/a_1 : s = \pm n + im, \quad \pm n - im.$

The solutions are obtained by substitution of $m_1 = m$, $m_2 = -m$ and $n_2 = n_1 = n$ into equation (27) and (28) and into equations (29–40).

(2) $\beta = a_0/a_1$: double roots $s = \pm n, \quad \pm n.$

For this particular case the inversion integrals are of the type

$$\int_{-\infty}^{\infty} \frac{dx}{(x-x_0)^2}. \tag{68}$$

It is well known that an integral of the type (68) does not exist even in the sense of a Cauchy principal value. It was discussed in [9] that such nonexistence of a solution implies a resonance, in the sense that the amplitude of the displacement becomes unbounded all along the beam. The value of the load velocity parameter β which yields an integral of the type (68) defines the first critical velocity. It was pointed out in [5] that this velocity is equal to the minimum phase velocity under which a free wave with a real wave number can be propagated along the beam.

(3) $a_0/a_1 < \beta < 1 : s = \pm n_1, \quad \pm n_2.$

In this velocity interval the integrand of the inversion integral has simple poles on the real axis. The integral can be evaluated by making the convention that the integration is not exactly along the real axis, but is along a line an infinitesimal amount above or under the real axis [14]. The two integrations give results that are valid respectively behind or in front of the load. It is not possible to ascertain which poles should be passed in the upper half-plane and which should be passed in the lower half-plane. As a result a question of uniqueness arises. This ambiguity is avoided however by considering the beam on the elastic foundation as a limit case of the beam on the damped foundation. As is discussed next, we can then immediately derive the solutions from the general expressions (27) and (28).

If $\xi \neq 0$ the roots for s are complex; for $\xi = 0$ the roots are real. If an infinitesimal amount of damping is introduced the roots are complex with a very small imaginary part. According to Table 1 the roots are of the type $s = \pm n_1 + im_1$ and $s = \pm n_2 + im_2$, where for small damping m_1 and m_2 are small. It can be shown that $n_2 > n_1$ if $m_2 > 0$ and $m_1 < 0$. It is essential to know the sign of the imaginary parts of the roots, because according to equation (20) this sign determines whether the term contributes to the head or to the tail wave. If the roots are now of the type $s = \pm n_1, \pm n_2$, the relative magnitudes of n_1 and n_2 indicate how the solutions for $\psi(R)$ and $W(R)$ can be derived from (27) and (28). We set $m_1 = m_2 = 0$, but we set $\operatorname{sgn}(m_2) = +1$ and $\operatorname{sgn}(m_1) = -1$ if $n_2 > n_1$. Also introducing $m_1 = m_2 = 0$ in the constants the rotation is obtained as

$$\frac{a_1^2}{F^*}\psi = A\cos(n_1 R)H(-R) - B\cos(n_2 R)H(R) \tag{69}$$

where

$$A = \left(\frac{2E_2}{E_1}\right)_{m_1=m_2=0} = \frac{1}{(n_1^2-n_2^2)(1-\beta^2)(\lambda^2-\beta^2)} \tag{70}$$

$$B = \left(\frac{2F_2}{F_1}\right)_{m_1=m_2=0} = \frac{-1}{(n_1^2-n_2^2)(1-\beta^2)(\lambda^2-\beta^2)}. \tag{71}$$

Similarly the deflexion is obtained from (28) as

$$\frac{a_1^2}{F^*} W = C\sin(n_1 R)H(-R) - D\sin(n_2 R)H(R) \tag{72}$$

where

$$C = \left(\frac{2G_3}{G_1}\right)_{m_1=m_2=0} = \frac{1+(\lambda^2-\beta^2)n_1^2}{n_1(n_1^2-n_2^2)(1-\beta^2)(\lambda^2-\beta^2)} \tag{73}$$

$$D = \left(\frac{2H_3}{H_1}\right)_{m_1=m_2=0} = \frac{-[1+(\lambda^2-\beta^2)n_2^2]}{n_2(n_1^2-n_2^2)(1-\beta^2)(\lambda^2-\beta^2)}. \tag{74}$$

It is of interest to investigate the solutions as β approaches unity. For $\beta \to 1$, $J^{\frac{1}{2}}$ can be expressed as

$$J^{\frac{1}{2}} \sim (\lambda^2-\beta^2-a_1^2\beta^2) - 2a_1^2(1-\beta^2)(\lambda^2-\beta^2)/(\lambda^2-\beta^2-a_1^2\beta^2). \tag{75}$$

If $n_2 > n_1$, it is seen from equations (65) and (75) that for β approaching unity n_1 remains finite, while n_2 increases as $1/(1-\beta^2)^{\frac{1}{2}}$. From equations (69–71) it then follows that the amplitude of $\psi(R)$ remains finite, but the wave number increases beyond bounds ahead of the load. It is also observed from (72–74) that both the amplitude and the wave number of the displacement head-wave increase beyond bounds. The term leading resonance is used to designate the type of resonance that occurs only ahead of the load. Since the bending moment is proportional to the derivative of the rotation ψ it can be checked that the bending moment exhibits leading resonance as β approaches unity. The value $\beta = 1$ corresponds to a load moving with a velocity $v = c_2$, where $c_2 = (\varkappa' G/\rho)^{\frac{1}{2}}$ is the propagation velocity of shear force disturbances in a free beam.

(4) $\quad 1 < \beta < \lambda : s = \pm im, \quad \pm n.$

For small damping the roots in this velocity interval are of the form $s = im_2$, $s = im_3$ and $s = \pm n_1 + im_1$, where m_1 is very small and negative. The solutions for the case $\zeta = 0$ are derived from (42) and (43) by setting $n_1 = n$, $m_1 = 0$, $m_2 = -m$, $m_3 = m$ and $\operatorname{sgn}(m_1) = -1$. The results are:

$$\frac{a_1^2}{F^*}\psi = A'\cos(nR)H(-R) + B' e^{mR}H(-R) - B' e^{-mR}H(R) \tag{76}$$

and

$$\frac{a_1^2}{F^*} W = C' \sin(nR)H(-R) + D' e^{mR}H(-R) + D' e^{-mR}H(R) \tag{77}$$

where

$$A' = \frac{1}{(m^2+n^2)(1-\beta^2)(\lambda^2-\beta^2)} \tag{78}$$

$$B' = \frac{-1}{2(m^2+n^2)(1-\beta^2)(\lambda^2-\beta^2)} \tag{79}$$

$$C' = \frac{1+(\lambda^2-\beta^2)n^2}{n(m^2+n^2)(1-\beta^2)(\lambda^2-\beta^2)} \tag{80}$$

$$D' = \frac{-[1-(\lambda^2-\beta^2)m^2]}{2m(m^2+n^2)(1-\beta^2)(\lambda^2-\beta^2)}. \tag{81}$$

For physically significant values of λ and a_1^2 the real roots for s, $s = \pm n$, remain finite while the values of the imaginary roots, $s = \pm im$, increase as $1/\sqrt{(\beta^2-1)}$ and $1/\sqrt{(\lambda^2-\beta^2)}$ respectively, as β approaches unity and λ. From (78) and (79) and (76) it follows that the amplitude of $\psi(R)$ remains finite in both cases. Equation (81) indicates that D' increases beyond bounds when β approaches unity, but vanishes when β approaches λ. According to equation (77) a resonance in displacement amplitude thus occurs as β approaches unity. However, because of the exponentials in equation (77) the resonance occurs only close to the origin. It can be checked that the bending moment displays the same type of localized resonance, not only when β approaches unity but also when β approaches λ inside the interval $1 < \beta < \lambda$. The value $\beta = \lambda$ corresponds to a load velocity equal to the propagation velocity of moment disturbances in a free beam.

(5) $\lambda < \beta : s = \pm n_1, \pm n_2.$

For small damping the roots are of the type $s = \pm n_1 + im_1$ and $s = \pm n_2 + im_2$, where m_1 and m_2 are small and negative. Substituting $m_2 = m_1 = 0$ and

$$\operatorname{sgn}(m_1) = \operatorname{sgn}(m_2) = -1$$

in (27) and (28) we obtain

$$\frac{a_1^2}{F^*} \psi = A \cos(n_1 R)H(-R) + B \cos(n_2 R)H(-R) \tag{82}$$

and

$$\frac{a_1^2}{F^*} W = C \sin(n_1 R)H(-R) + D \sin(n_2 R)H(-R) \tag{83}$$

where the constants A, B, C and D are defined by equations (70–74). It is noticed that if β approaches λ the larger of the roots, say n_2, approaches infinity as $1/\sqrt{(\beta^2-\lambda^2)}$. Inspection of equations (70–74) shows that the amplitude of the rotation remains finite. The amplitude of the displacement, however, shows a trailing resonance. The bending moment also exhibits a trailing resonance.

7. DISCONTINUITIES UNDER THE MOVING LOAD

Discontinuities under the moving load can be detected by considering the equations of motion (11) and (12). By eliminating $\psi(R)$ the equation for $W(R)$ is obtained as

$$a_1^2(1-\beta^2)(\lambda^2-\beta^2)W^{IV}+2a_1\beta\xi(\lambda^2-\beta^2)W'''-(\lambda^2-\beta^2-a_1^2\beta^2)W''$$
$$-2a_1\beta\xi W'+W = F^*\delta(R)-(\lambda^2-\beta^2)F^*\delta''(R). \tag{84}$$

Similarly the equation for $\psi(R)$ is obtained as

$$a_1^2(1-\beta^2)(\lambda^2-\beta^2)\psi^{IV}+2a_1\beta\xi(\lambda^2-\beta^2)\psi'''-(\lambda^2-\beta^2-a_1^2\beta^2)\psi''$$
$$-2a_1\beta\xi\psi'+\psi = F^*\delta'(R). \tag{85}$$

Denoting a discontinuity by $S[\;]$, we obtain by integrating equation (84)

$$S[W'] = -F^*/a_1^2(1-\beta^2). \tag{86}$$

Also by integrating equation (85)

$$S[\psi''] = F^*/a_1^2(1-\beta^2)(\lambda^2-\beta^2). \tag{87}$$

The results (86) and (87) indicate that the displacement, the rotation and the bending moment are continuous. The discontinuities (86) and (87) can also be checked directly from the expressions for $\psi(R)$ and $W(R)$.

It is of note that the discontinuities are independent of the damping coefficient ξ. Thus also for the beam on the damped foundation the discontinuity in W' increases beyond bounds when β approaches unity. The discontinuity in ψ'' becomes unbounded when β approaches unity or λ.

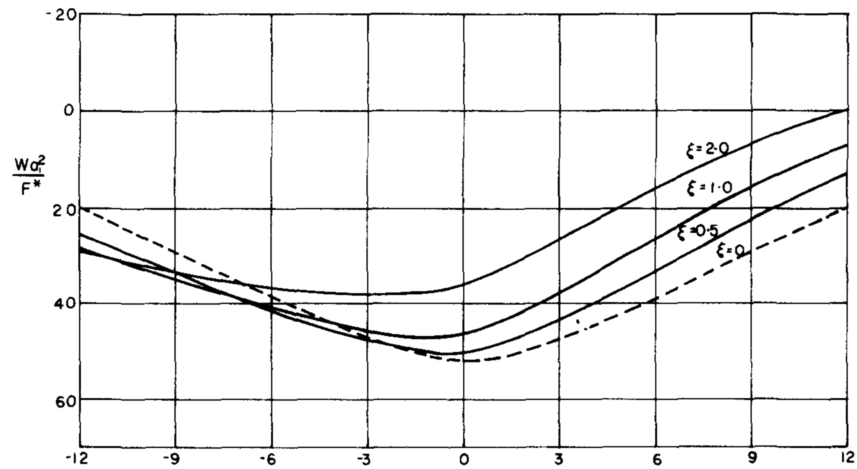

FIG. 4. Beam deflexion, $\beta = 0{\cdot}1$, $a_1^2 = 1000$, $\lambda^2 = 3$.

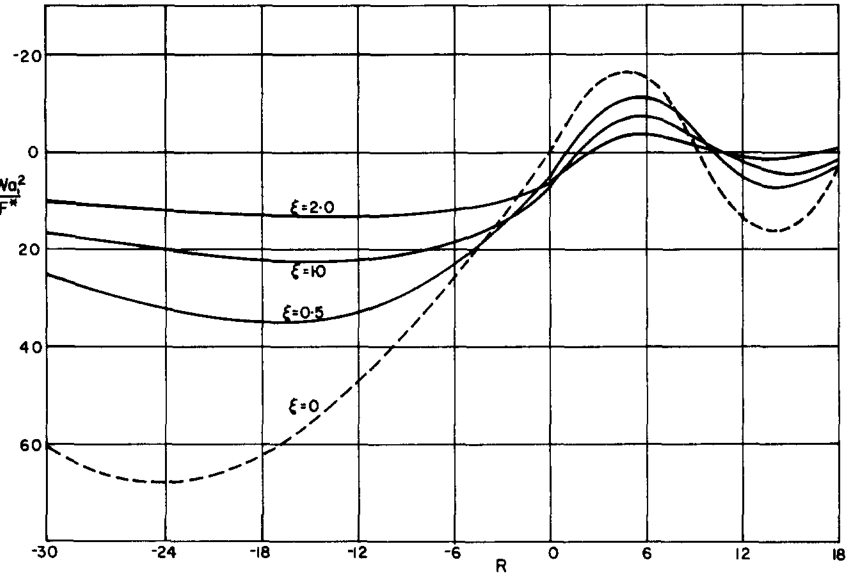

FIG. 5. Beam deflexion, $\beta = 0{\cdot}5$, $a_1^2 = 1000$, $\lambda^2 = 3$.

8. NUMERICAL RESULTS

For several values of the damping parameter ξ and the velocity parameter β the displacement and the bending moment are plotted as functions of R. In all cases numerical values for λ and a_1^2 were selected as $\lambda = \sqrt{3}$ and $a_1^2 = 1000$.

In Fig. 4 the displacement is shown for subcritical load velocity and for various values of the damping parameter. Whereas the displacement for the elastic foundation is symmetric relative to the load, the maximum is behind the load for a damped foundation.

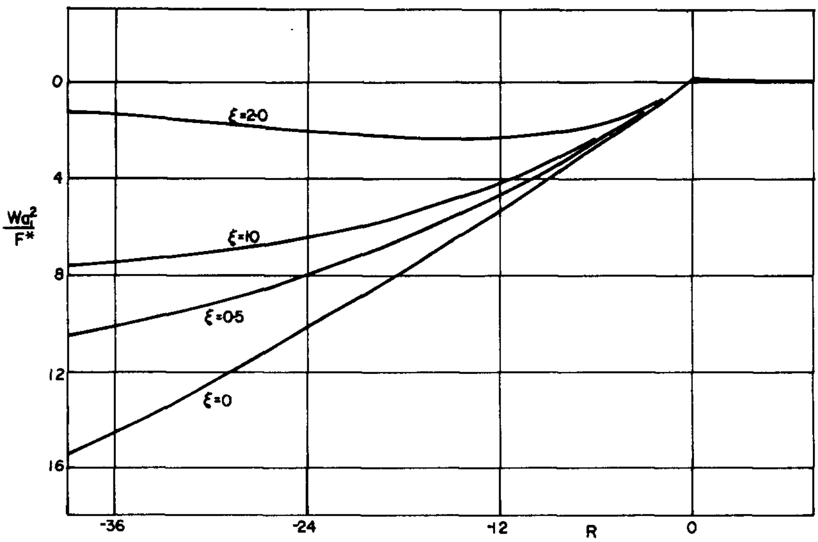

FIG. 6. Beam deflexion, $\beta = 1{\cdot}5$, $a_1^2 = 1000$, $\lambda^2 = 3$.

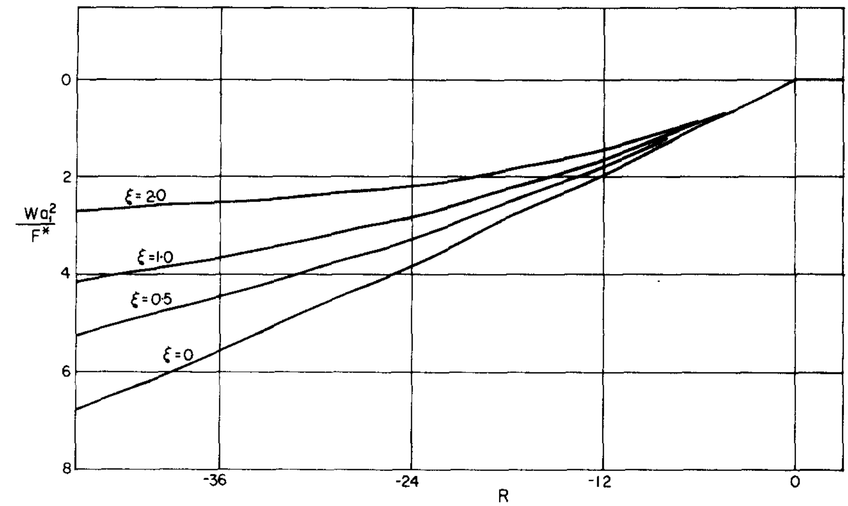

FIG. 7. Beam deflexion, $\beta = 2{\cdot}5$, $a_1^2 = 1000$, $\lambda^2 = 3$.

In Fig. 5 displacement curves are shown for a load velocity higher than the first critical velocity. The undamped foundation $\xi = 0$, gives undamped sinusoids. It is noticed that in this load–velocity range the damping has a more pronounced influence on the deflexion amplitude than at subcritical velocities. For load velocities higher than the propagation velocity of shear force disturbances the deflexion curves have again undergone a difference in appearance. It should be mentioned that the deflexion behind the load is still periodic, but the wavelength is beyond the range of Fig. 6. For load velocities higher than the propagation speed of moment disturbances the beam is undisturbed ahead of the

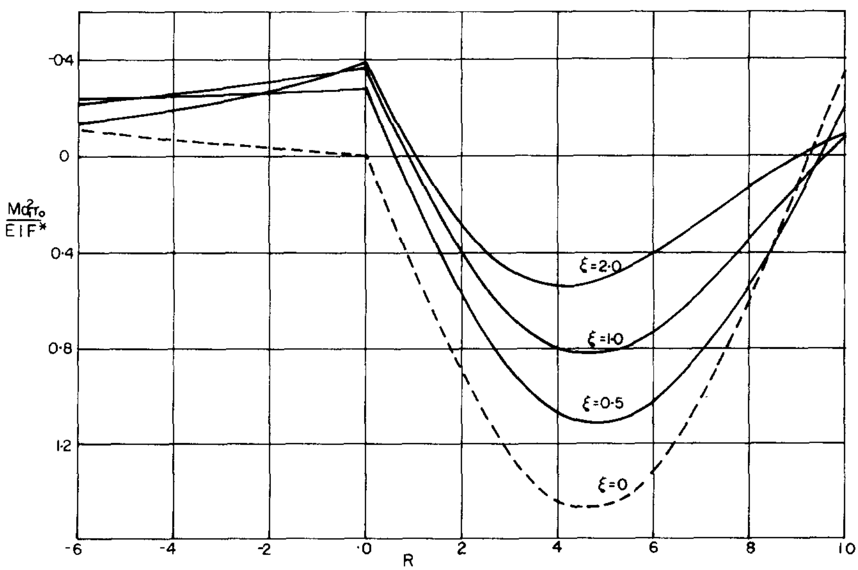

FIG. 8. Bending moment, $\beta = 0{\cdot}5$, $a_1^2 = 1000$, $\lambda^2 = 3$.

load, Fig. 7. Attention is drawn to the differences in the scales that were used to plot the deflexions in Fig. 4, Fig. 5, Fig. 6 and Fig. 7 respectively. The bending moment is shown in Fig. 8 for various values of the damping parameter, and in Fig. 9 for $\xi = 0{\cdot}5$ and various load velocities.

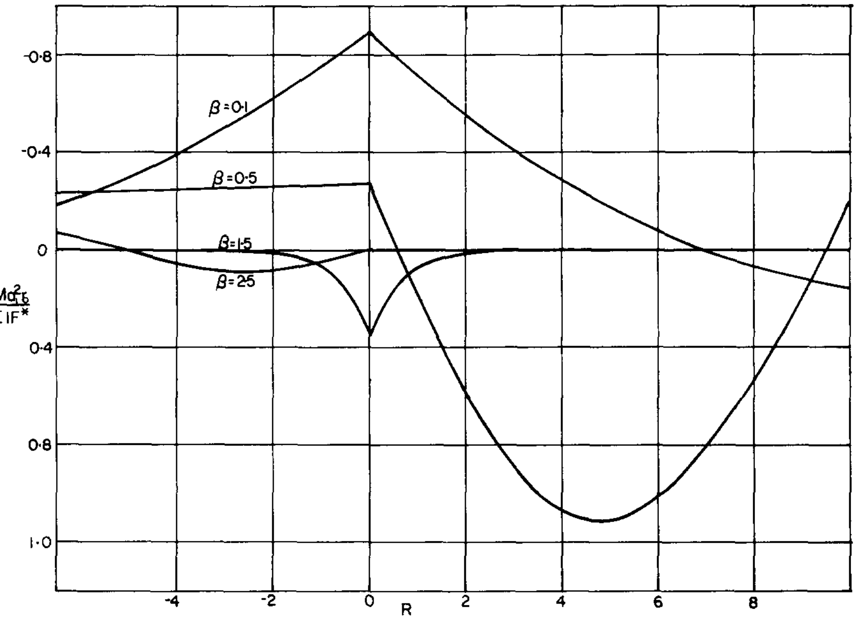

FIG. 9. Bending moment, $\xi = 0{\cdot}5$, $a_1^2 = 1000$, $\lambda^2 = 3$.

9. CONCLUSIONS

It has been shown that transverse foundation damping decreases the magnitudes of the displacement and the bending moment. The discontinuities under the load in the slope of the displacement and the second derivative of the rotation are not affected by transverse foundation damping.

In this paper the Complex Fourier Transform has been found a convenient method of analysis. Due to the foundation damping the transformed quantities possessed poles in the complex plane, never on the real axis. The favorable positions of the poles made the inversion process straightforward and questions of uniqueness did not arise. By considering the elastic foundation as a limitcase the zero damping response can also be obtained without ambiguity.

Acknowledgement—The results presented in this paper were obtained in the course of research sponsored by the Air Force Office of Scientific Research under Grant AF-AFOSR-100-64. The authors are grateful to Professor George Herrmann for suggesting the problem.

REFERENCES

[1] B. K. HOVEY, Beitrag zur Dynamik des geraden Eisenbahngleises, Dissertation, Göttingen (1933).
[2] K. LUDWIG, Die Verformung eines beiderseits unbegrenzten elastisch gebetteten Gleises durch Lasten mit Konstanter Horizontalgeschwindigkeit, *Proc. 5th Int. Cong. Appl. Mech., Cambridge, Mass.*, p. 650 (1938).

[3] J. DÖRR, *Ing. Arch.* **14**, 167 (1943).
[4] P. M. MATHEWS, *Z. Angew. Math. Mech.* **38**, 105 (1958).
[5] S. H. CRANDALL, The Timoshenko beam on an elastic foundation, *Proc. 3rd Midwestern Conf. Solid Mech.*, p. 146 (1957).
[6] J. MIKLOWITZ and J. R. LLOYD, *J. Appl. Mech.* **29**, 459 (1962).
[7] J. T. KENNEY JR., *J. Appl. Mech.* **21**, 359 (1954).
[8] P. M. MATHEWS, *Z. Angew. Math. Mech.* **39**, 13 (1959).
[9] P. G. BUTA and J. P. JONES, *J. Appl. Mech.* **31**, 105 (1964).
[10] S. C. TANG, Dynamic response of a thin-walled cylindrical tube under internal moving pressure, Ph.D. Dissertation, The University of Michigan (Jan. 1963).
[11] A. W. PANTON and W. S. BURNSIDE, *The Theory of Equations* (3rd Ed.) Art 68. Hodges Figgis, Dublin (1892).
[12] E. J. ROUTH, *Advanced Dynamics of a System of Rigid Bodies* (6th Ed.) Chapter VI. Dover, New York.
[13] R. D. MINDLIN and H. DERESIEWICZ, Timoshenko's shear coefficient for flexural vibrations of beams, *Proc. 2nd U.S. National Congress of Appl. Mech.*, p. 175 (1954).
[14] P. M. MORSE, *Vibration and Sound*, p. 15. McGraw-Hill, New York (1948).

(*Received* 15 *October* 1964)

Résumé—Une poutre uniforme, de longueur infinie, est soumise à une force dont le point d'application se déplace avec une vitesse longitudinale constante. L'auteur obtient des solutions qui sont invariantes, par rapport au temps, dans un système de coordonnées se déplaçant à la vitesse de la charge. La résistance à la charge comprend l'effet d'amortissement. L'auteur étudie l'influence du coefficient d'amortissement et de la vitesse de la charge sur la réaction de la poutre. Il examine aussi le cas limite d'un amortissement nul et il fait apparaître l'influence des différents cas de résonance.

Абстракт—На балку постоянного сечения бесконечной длины действует сила, точка приложения которой перемещается по балке с постоянной скоростью. Получаемые решения непостоянны во времени в координатной системе, движущейся со скоростью нагрузки. Несущее устройство заключает в себе демпфирующие действия. Рассматривается влияние коэффициента демпфирования и скорости нагрузки на реакцию балки. Включается предельный случай нулевого демпфирования и освещаются различные резонансные эффекты.